AFRL-RX-WP-TP-2008-4310

MICROSTRUCTURAL INFLUENCES ON VERY HIGH CYCLE FATIGUE CRACK INITIATION IN Ti-6246 (PREPRINT)

C.J. Szczepanski, S.K. Jha, J.M. Larsen, and J.W. Jones

Metals Branch
Metals, Ceramics, and NDE Division

APRIL 2008

AIR FORCE RESEARCH LABORATORY
MATERIALS AND MANUFACTURING DIRECTORATE
WRIGHT-PATTERSON AIR FORCE BASE, OH 45433-7750
AIR FORCE MATERIEL COMMAND
UNITED STATES AIR FORCE

REPORT DOCUMENTATION PAGE

Form Approved
OMB No. 0704-0188

1. REPORT DATE *(DD-MM-YY)*	2. REPORT TYPE	3. DATES COVERED *(From - To)*
April 2008	Journal Article Preprint	

4. TITLE AND SUBTITLE

MICROSTRUCTURAL INFLUENCES ON VERY HIGH CYCLE FATIGUE CRACK INITIATION IN Ti-6246 (PREPRINT)

5a. CONTRACT NUMBER
In-house

5b. GRANT NUMBER

5c. PROGRAM ELEMENT NUMBER
62102F

6. AUTHOR(S)

C.J. Szczepanski and J.W. Jones (University of Michigan)
S.K. Jha (Universal Technology Corporation)
J.M. Larsen (AFRL/RXLMN)

5d. PROJECT NUMBER
4347

5e. TASK NUMBER
RG

5f. WORK UNIT NUMBER
M02R3000

7. PERFORMING ORGANIZATION NAME(S) AND ADDRESS(ES)

University of Michigan

Universal Technology Corporation

Metals Branch (AFRL/RXLMN)
Metals, Ceramics, and NDE Division
Materials and Manufacturing Directorate
Wright-Patterson Air Force Base, OH 45433-7750
Air Force Materiel Command, United States Air Force

8. PERFORMING ORGANIZATION REPORT NUMBER
AFRL-RX-WP-TP-2008-4310

9. SPONSORING/MONITORING AGENCY NAME(S) AND ADDRESS(ES)

Air Force Research Laboratory
Materials and Manufacturing Directorate
Wright-Patterson Air Force Base, OH 45433-7750
Air Force Materiel Command
United States Air Force

10. SPONSORING/MONITORING AGENCY ACRONYM(S)
AFRL/RXLMN

11. SPONSORING/MONITORING AGENCY REPORT NUMBER(S)
AFRL-RX-WP-TP-2008-4310

12. DISTRIBUTION/AVAILABILITY STATEMENT
Approved for public release; distribution unlimited.

13. SUPPLEMENTARY NOTES
Journal article submitted to *Metallurgical and Materials Transactions*.

PAO Case Number: WPAFB 08-0956; Clearance Date: 14 Mar 2008. The U.S. Government is joint author of this work and has the right to use, modify, reproduce, release, perform, display, or disclose the work. Paper contains color.

14. ABSTRACT

The fatigue behavior of an alpha+beta titanium alloy, Ti-6Al-2Sn-4Zr-6Mo, has been characterized in the very high cycle fatigue (VHCF) regime using ultrasonic fatigue (20 kHz) techniques. Stress levels of 40 to 60% of the yield strength of this alloy have been examined. Fatigue lifetimes in the range of 10 (to the 6th) to 10 (to the 9th) cycles are observed and fatigue cracks initiate from both surface and subsurface sites. This study examines the mechanisms of fatigue crack formation by quantifying critical microstructural features observed in the fatigue crack initiation region. The fracture surface near the fatigue crack initiation site was crystallographic in nature. Facets, which result from the fracture of primary alpha grains, are associated with the crack initiation process. The primary alpha grains that form facets are typically larger in size than average. The spatial distribution of primary alpha grains relative to each other observed near the initiation site did not correlate with fatigue life. Furthermore, the spatial distribution of primary alpha grains did not provide a suitable means for discerning crack initiation sites from randomly selected nominal areas.

15. SUBJECT TERMS
fatigue, titanium alloy, very high cycle fatigue, crack formation, microstructure

16. SECURITY CLASSIFICATION OF:			17. LIMITATION OF ABSTRACT:	18. NUMBER OF PAGES	19a. NAME OF RESPONSIBLE PERSON (Monitor)
a. REPORT	b. ABSTRACT	c. THIS PAGE			James M. Larsen
Unclassified	Unclassified	Unclassified	SAR	28	19b. TELEPHONE NUMBER *(Include Area Code)* N/A

Standard Form 298 (Rev. 8-98)
Prescribed by ANSI Std. Z39-18

Microstructural Influences on Very High Cycle Fatigue Crack Initiation in Ti-6246

C. J. Szczepanski[1,3]; S. K. Jha[2]; J. M. Larsen[3]; J. W. Jones[1]
[3]Air Force Research Laboratory, Materials and Manufacturing Directorate,
AFRL/RXLMN, Wright-Patterson AFB, OH-45433 USA
[1]University of Michigan, Materials Science and Engineering, Ann Arbor, MI-48109 USA
[2]Universal Technology Corporation, Dayton, Ohio 45432 USA

The fatigue behavior of an alpha + beta titanium alloy, Ti-6Al-2Sn-4Zr-6Mo, has been characterized in the very high cycle fatigue (VHCF) regime using ultrasonic fatigue (20 kHz) techniques. Stress levels (σ_{max}) of 40-60% of the yield strength of this alloy have been examined. Fatigue lifetimes in the range of 10^6 to 10^9 cycles are observed and fatigue cracks initiate from both surface and subsurface sites. This study examines the mechanisms of fatigue crack formation by quantifying critical microstructural features observed in the fatigue crack initiation region. The fracture surface near the fatigue crack initiation site was crystallographic in nature. Facets, which result from the fracture of primary alpha (α_p) grains, are associated with the crack initiation process. The α_p grains that form facets are typically larger in size than average. The spatial distribution of α_p grains relative to each other observed near the initiation site did not correlate with fatigue life. Furthermore, the spatial distribution of α_p grains did not provide a suitable means for discerning crack initiation sites from randomly selected nominal areas. Stereo fractography measurements have shown that the facets observed at or near the initiation sites are oriented for slip, i.e. they are oriented close to 45° with respect to the loading axis. Orientation imaging microscopy (OIM) indicates that these facets form on the basal plane of α_p grains. Furthermore, a large majority of the grains and laths near the site of crack initiation are preferentially oriented for either basal or prism slip. Thus, crack initiation is believed to occur in regions where α_p grains and α laths have similar crystallographic orientations. Nominal microstructural areas are characterized to determine the prevalence of regions containing similarly oriented α_p grains. The presence of textured regions at the crack initiation site is used to explain the process of fatigue crack initiation that accounts for microstructural heterogeneity. This explanation hypothesizes that slip accumulates within a textured region by basal and prism slip in similarly oriented α_p grains.

I. INTRODUCTION

The study of very high cycle fatigue (VHCF) behavior is attracting increased interest from industry, since many components in structural applications such as automobile cylinder heads, engine blocks[1] and turbine engines will accumulate 10^8 to 10^{10} cycles in service. The conventional approach of designing components to a fatigue limit is not applicable in VHCF, since fatigue failures have been observed[2] below the conventional fatigue limit. This has led some researchers[3] to propose a modified SN curve where surface initiated fatigue failures are observed at high stresses and subsurface fatigue crack initiation is observed at very long lifetimes below the conventional fatigue limit. Mughrabi[4] explained failures below the conventional fatigue limit in terms of fundamental physical mechanisms of fatigue damage accumulation by suggesting that even though macroscopic strain in VHCF is below the PSB threshold, slip irreversibility can still accumulate and lead to failure. This agrees with the work of Lukáš and Kunz[5]

who argue that in the VHCF regime the applied strain is nominally elastic and only localized plastic deformation will accumulate at specific microstructural locations. Thus, as compared to LCF where the majority of grains accommodate some plastic deformation, in HCF and VHCF it is likely that specific microstructural configurations can be associated with more rapid local fatigue damage accumulation. Such fatigue critical microstructural neighborhoods have been defined based on grain size,[9] spatial orientation,[9,10] proximity to the specimen surface,[3,6] and crystallographic orientation.[7,17] The current work examines which of these factors, if any, contribute to the process of fatigue crack initiation in α + β titanium alloys.

Much of the literature on fatigue crack initiation in α + β titanium alloys focuses on analysis of the fracture surfaces to determine the deformation and possible strain accumulation mechanisms that are responsible for crack initiation. In materials that do not contain inclusions or porosity, fatigue cracks will initiate in locations where the local microstructure promotes the accumulation of irreversible slip. Hall's review[8] of fatigue crack initiation in α + β titanium alloys establishes that fatigue damage typically accumulates in the alpha phase. Further, the length scale of the deformation will vary depending on the microstructure and processing conditions. Fatigue critical microstructural features have been identified as individual α_p grains, α colonies, prior β grains, or regions of similarly oriented α grains. Mahajan and Margolin[9] found that in Ti-6246 fatigue cracks initiated in large alpha grains or in areas where a number of alpha grains were clustered together that presumably increased the slip length. They hypothesized that a likely method for improving the fatigue resistance of this alloy is to increase the spacing between alpha grains or to refine the α_p grain size to limit slip transmission between α_p grains or plastic deformation within grains, respectively. Researchers have investigated clustering both in a statistical[10] and a micro-mechanistic[11] approach. Ravi Chandran and Jha[10] determined that α_p clustering is the fatigue critical microstructural feature in Ti-10V-2Fe-3Al in one population of failures, and they were able to model this using Poisson defect statistics. In Waspaloy, Davidson et. al.[11] found that the crack initiation sites are associated with clusters of similarly-oriented grains, which they termed "supergrains." They suggested that supergrains were more susceptible to fatigue crack initiation because localized deformation in one grain could be more easily accommodated in adjacent grains due to their similar crystallographic orientation. Regions of material with similar crystallographic orientation are commonly observed to initiate fatigue cracks in titanium alloys, as well.[7,8,17,12] Bieler and Semiatin[13] established that the presence of these microtextured regions results from local heterogeneities in deformation during thermomechanical processing.

Macroscopic textures, resulting from the processing history of titanium alloys, are known to influence mean fatigue properties.[14,15] However, in the regime of VHCF, damage accumulation will only occur if the local microstructure is suitable for irreversible slip to accumulate. In other words, microstructural heterogeneity is thought to cause scatter in fatigue lifetimes. Evidence of such behavior has been observed by a number of researchers who have investigated the effect of local texture on fatigue crack initiation[7,17] and propagation[16] in titanium alloys. In Ti-6242, Sinha et. al.[17] have found that dwell fatigue loading, in which specimens are held at a static load as part of every fatigue cycle, leads to crack formation in microtextured regions suitable for basal slip that are surrounded by regions of material oriented for prism slip. Multiple cracks

initiated and while the dominant crack was not necessarily the first to initiate, it did grow out of the largest microtextured region. In the work of LeBiavant et. al.[7] numerous cracks were found to initiate in macrozones where the majority of α_p grains were oriented for basal or prism slip. Each of these studies aims to understand the contribution of heterogeneous texture to the initiation and growth of fatigue cracks in the high cycle fatigue (HCF) regime. The objective of this work is to establish which microstructural features and configurations cause fatigue crack initiation in the VHCF regime to better understand the mechanisms of damage accumulation and fatigue crack initiation.

II. MATERIALS AND EXPERIMENTAL PROCEDURES

The material used in this study is Ti-6Al-2Sn-4Zr-6Mo (wt%), which is commonly referred to as Ti-6246. Typical processing conditions[18] were used to produce bimodal microstructures consisting of equiaxed alpha grains in a transformed beta matrix, as shown in Figure 1. The average α_p grain size measured using the linear intercept method is 3.7 μm ± 2.6 μm. As Figure 2 shows, the α_p grain size follows a log-normal distribution. The area fraction of α_p grains is approximately 30%, and within the transformed beta regions, the area fraction of lath α was measured as 50%, resulting in a total area fraction of alpha near 65% (30% α_p and 35% lath α). Area fractions were measured using the point count method and verified with commercially available computational image analysis tools. The yield stress of this material is 1160 MPa.

Specimens were cut circumferentially from a forged pancake that was processed to simulate forging conditions in an actual component. Cylindrical specimen blanks were cut from this material, and grip ends of Ti-6Al-4V rod were inertia welded onto the specimen blanks. Final machining of cylindrical specimens was completed by low stress grinding to minimize compressive residual stresses.[19] All specimens were then electropolished to remove the remaining surface compressive residual stresses. The gage was 4 mm in diameter and 12 mm in length. Axial fatigue testing was completed using ultrasonic fatigue techniques that are detailed elsewhere.[20,21,22] Specimens were designed such that their resonant frequency was approximately 20 kHz.

Observation of the fracture surfaces was completed using two scanning electron microscopes: a Leica Cambridge S360FE microscope operating at a probe current of 100 pA and accelerating voltage of 20 kV and a Phillips XL30FEG operating at 10 kV with a probe current of approximately 2 nA. Orientation imaging microscopy (OIM) was completed on polished sections of the fractured fatigue specimens using these two microscopes with detectors manufactured by EDAX-TSL. For the OIM investigations, the probe current and accelerating voltage were approximately 10 nA and 20 kV, respectively.

OIM scans were completed on the region of material just below the fracture surfaces at the site of fatigue crack initiation. The section of material that was exposed for OIM analysis is depicted as plane B-B in Figure 3**.** Figure 3 also illustrates the reference frame for OIM scans. The OIM scans have been acquired in the RD-TD plane with RD corresponding to the tensile axis of the fatigue specimens. The advantage of sectioning samples to expose this plane is that the fracture surface and the microstructure just below the crack initiation site can be viewed simultaneously. These pieces containing the fracture surface were then mounted in epoxy and mechanically polished. Material removal depth was monitored with a micrometer. As the desired plane for observation

was approached, the specimen was placed in a vibratory polisher to perform a final low-stress polishing in a 0.05 μm solution of colloidal silica. This final polishing step was critical to the acquisition of reliable OIM data. The epoxy mount was then dissolved in acetone to allow simultaneous imaging in the SEM of the fracture surface and the polished section below the site of crack initiation.

To gain insight into the process of crack initiation, the spatial orientation of facets was measured with respect to the loading axis using stereology. Images used to produce 3D reconstructions of fracture surfaces were acquired in the SEM by centering the feature of interest in the field of view at the eucentric height. Images were then acquired at tilt angles of 0° and 6° with respect to the stage normal position for each facet. The technique and procedure for generating stereo pairs was validated using MeX commercial software (Alicona: Grambach, Austria) on known geometries such as Vickers microhardness indents.

III. RESULTS AND DISCUSSION

Fatigue lifetime

Fatigue failures in the range of 10^6 to 10^9 cycles were observed, as shown in Figure 4. Cracks initiated from surface and subsurface locations, as indicated by the open and closed data points, respectively. Data are shown for the two frequencies investigated; 20 Hz and 20 kHz and all tests were run at a load ratio of 0.05. The 20 Hz tests were conducted at stress levels (σ_{max}) of 820 MPa and higher at AFRL.[23] Ultrasonic frequency fatigue testing was completed at 20 kHz at stresses (σ_{max}) of 700 MPa and below.[24] Although the stress levels do not overlap, the data follow the same trend as expected for a typical SN curve. This indicates that there is no appreciable frequency effect on fatigue lifetime between testing frequencies of 20 kHz and 20 Hz. This is consistent with the findings of Paparikicou et. al.,[25] who also observed a negligible effect of test frequency on the fatigue lifetimes of an α+β titanium alloy.

Additionally, there is an increased likelihood of subsurface crack initiation as the stress level is decreased, which is also consistent across the testing frequencies. At ultrasonic frequencies, surface crack initiation was observed approximately 80% of the time for the highest stress level investigated (700 MPa), while at the lowest stress level (550 MPa), only 20% of the specimens failed from a surface initiated fatigue crack. Specimens that failed by surface crack initiation typically tended to have shorter lifetimes than those that failed from subsurface crack initiation. However, in a few cases, surface initiated failures were observed to have similar lifetimes as specimens that failed from subsurface crack initiation sites, as has been observed in other investigations of fatigue in α + β titanium alloys.[35]

Fractography

Fractographs of typical crack initiation sites in surface and subsurface locations are compared in Figure 5. In all cases, facets are observed at the site of crack initiation and their size is commensurate with the larger α_p grains. The facets are presumed to form by the fatigue fracture of α_p grains along a preferred crystallographic plane and are referred to here as α_p facets. The average α_p grain size is approximately 4 μm, while the average facet size is 5.3 μm. The histogram of α_p facet size is overlaid on the α_p grain size histogram in Figure 2. The α_p facet sizes were measured from SEM micrographs, and it

is noted that facets are actually three dimensional features projected onto a 2D micrograph; i.e. the true size of the facets is larger than is represented in the histogram.

Failed specimens have been classified into three categories based on the appearance of the fracture surface near the crack initiation site: surface, isolated subsurface faceting, and macroscopically planar subsurface sites. In the case of surface crack initiation and subsurface crack initiation with isolated facets, individual α_p facets are observed on the fracture surface, as shown in Figure 5 (a) and (b), respectively. Figure 5 (c) illustrates the third type of crack initiation site, which consists of a macroscopically planar region that is occasionally observed in subsurface crack initiation. This type of crack initiation spans a number of α_p grains and transformed β regions and the crack appears to form along the same plane relative to the loading axis in each of these grains. Upon closer inspection of these initiation sites, evidence of ductility is apparent within these large flat regions. Thus it is not appropriate to call them facets since they are not truly planar. Crack initiation was classified as surface if the α_p facets intersected the specimen surface. Figure 6 displays the fatigue lifetimes where the data points have been classified into three different groups. Surface crack initiation generally leads to the shortest lifetimes. However, the lifetimes of specimens failing by the two types of subsurface crack initiation mechanisms are not significantly different.

Subsurface crack initiation has been observed in a number of fatigue studies on $\alpha + \beta$ titanium alloys.[10,23,32,33,34,35] The competition between surface and subsurface crack initiation sites has alternately been attributed to the specimen surface to volume ratio,[27] the presence of compressive residual stresses on the surface,[34] environmental effects,[26] and the relative ease with which grains can deform at a free surface as compared to the specimen interior.

In the regime of VHCF, only certain microstructural neighborhoods are susceptible to fatigue damage accumulation that leads to crack initiation, and these microstructural configurations do not necessarily exist at the specimen surface. This idea was first put forth by Mughrabi,[27] and Jha and Larsen[28] subsequently proposed that different microstructural neighborhoods may be in competition with one another to initiate the dominant fatigue crack. In the current work, it appears that there may be a number of different microstructural regions in each sample that may initiate a fatigue crack, however only the site that accumulates fatigue damage most rapidly will ultimately lead to fatigue crack initiation. The fact that three characteristic crack initiation sites have been observed at the same stress level indicates that there is competition between different microstructural neighborhoods for crack initiation. The evidence suggests that if there is not a suitable group of α_p grains near the specimen surface, then a crack will initiate from the specimen interior, and the presence of different microstructural neighborhoods in the interior will cause either a subsurface initiation site with isolated facets or with a macroscopically planar region. The occurrence of α_p facets at the crack initiation sites indicates that α_p grains are influential in accumulating fatigue damage and subsequent fatigue crack initiation. Similar observations led to speculation[29] that specific spatial and crystallographic orientations of α_p grains are required for fatigue cracks to initiate.

Spatial clustering of α_p grains

As illustrated by the highlighted features in Figure 7, there is a higher tendency of faceted fracture of α_p grains near the site of fatigue crack initiation. To characterize the spatial distribution of α_p grains and whether this influenced fatigue crack initiation in the current work, the area fraction of α_p facets was measured from fracture surfaces. The results are shown in Figure 8, where the area fraction of the fracture surface covered by facets is plotted as a function of the crack tip driving force. The stress intensity values on the abscissa were calculated using the Newman Raju[30] stress intensity solutions for surface cracks while the Murakami[31] solutions were used for subsurface cracks. The thick bounding lines in the plot represent the extremes of α_p grain spatial orientation in the general microstructure, i.e. the most clustered regions and the regions nearly devoid of α_p grains. As larger areas are probed, the area fraction of α_p grains, which is represented by these bounding lines, converges to the global measurement of α_p area fraction of 27% as indicated by the horizontal dotted line. Open data points represent surface failures, while closed data points mark the area fraction of facets from specimens that failed by subsurface crack initiation. The legends in the plots indicate the lifetime of specimens that have been examined with this analysis. These data have been dissected in two different ways to examine the effects on faceting of surface vs. subsurface crack initiation and the effect of stress level. The plots in Figure 8(a) and (b) illustrate the area fraction of faceting in surface and subsurface initiated failures, respectively. Figure 8(c) displays the area fraction of facets with respect to the presumed crack size for specimens tested at 700 MPa (σ_{max}), while Figure 8(d) shows this data for specimens tested at 600 MPa (σ_{max}).

A number of observations can be drawn from these plots; firstly, the area fraction of α_p facets typically decreases as material farther from the crack initiation site is considered. Since the facet formation process is suspected to result from fracture of α_p grains along crystallographic directions favorable for slip, the apparent lack of faceting for large crack sizes is expected. The local microstructure is known to influence crack initiation and small crack growth, and therefore more facets are expected to form in these regions than in regions where long crack growth conditions apply.

The results suggest that there is no critical value of spatial clustering of α_p that must be met for cracks to initiate. In some cases, the α_p facets are much more dispersed at the site of crack initiation than the α_p grains are in the general microstructure, while in other samples the degree of faceting at the initiation site is markedly higher than the average α_p grain distribution. Thus, the spatial distribution of α_p grains alone does not determine where cracks will initiate in the general microstructure. Additionally, the lifetimes of specimens do not correlate with the spatial distribution of α_p at the crack initiation sites. This suggests that the area fraction of faceting does not indicate the rate of fatigue damage accumulation or degree of difficulty to initiate a fatigue crack in these microstructural regions. As the plots in Figure 8(a) and (b) illustrate, there is no discernable difference in the degree of faceting between surface and subsurface crack initiation. It is apparent that in general more faceting is observed at the crack initiation sites for higher stress levels of σ_{max} as shown in Figure 8(c) and (d). This finding may indicate that higher maximum stress will lead to higher resolved stresses on the basal and prism slip systems in unfavorably oriented grains. Thus, slip may be activated in grains that would not otherwise contribute to the damage accumulation process. Therefore, a

larger volume of material could contribute to the crack initiation process at higher stress levels.

Spatial Orientation of Facets

A number of researchers[32,33,34,35,36] have found that facets at the crack initiation site are typically oriented normal to the tensile axis. This led some researchers[35,36] to speculate that stress redistribution within the microstructure can lead to activation of a pseudo-cleavage mechanism of fatigue crack initiation in which it is proposed that grains oriented for slip may induce stress in adjacent grains. As the stress in this neighboring grain increases, it will eventually fail by a cleavage type failure mechanism. In the current study, the larger facets at the crack initiation site are typically oriented for slip (facet normal is inclined at an angle of greater than 30° with respect to the fracture surface plane). In Figure 9 the facets that have been measured by this technique are highlighted and the labels correspond to the numbers in Table I. Facets 1 and 2 have the ideal orientation for slip.

Specimens were sectioned to expose the microstructure below the crack initiation site. Figure 3 is a schematic that depicts the sectioning plane cutting through the crack initiation site. An SEM micrograph of a specimen that was prepared by this sectioning procedure is shown in Figure 10, which illustrates that the crack plane is not perpendicular to the loading axis at the crack initiation site. The tensile axis in this image is vertical in the plane of the page. From this image, it is apparent that the crack initiation process is caused by slip since this plane is oriented for a high resolved shear stress. These results indicate that for this alloy and test condition, fatigue cracks initiate by a slip process and not by pseudo-cleavage as observed in other investigations[36,17] of the fatigue behavior in alpha + beta titanium alloys.

Crystallographic Orientation of Crack Initiating Region

The crystallographic orientation of alpha grains at the site of crack initiation was determined using OIM on samples sectioned as shown schematically in Figure 3. Since the spatial orientation of the facets with respect to the tensile axis was known, OIM was used to determine which crystallographic planes corresponded to the facet planes. The facets observed on the fracture surface were determined to be basal planes of the equiaxed α_p grains. The inverse pole figure (IPF) map from an OIM scan is shown in Figure 11. The schematic illustrates the reference frame for this image. RD corresponds to the tensile axis, while ND is coming out of the plane of the page in this image. Although the micrograph displays the microstructure as viewed from the RD-TD plane, the orientations that these colors represent are shown from the perspective of viewing down the RD axis. The colors in the IPF map correspond to the colors in the unit triangle shown in the top right of the figure. The orientations of the four indicated features are also plotted in the unit triangle which displays the Schmid factor iso-curves for basal slip. These grains have high Schmid factors for basal slip, which indicates that the facets formed by slip on a basal plane. Table II lists the spatial orientation of facets with respect to the loading axis (RD) and the crystallographic angle with respect to the basal pole for each of the facets marked in the micrograph. As shown in Table II, the spatial and crystallographic angles follow the same trend and the facet normal is aligned with the basal pole of these grains. Facets have also been examined in surface failures, and the

facets form along the basal plane in a α_p grain oriented for slip. These results indicate that basal slip is operative in a number of grains at the crack initiation site, and this raises the question of how many α_p grains are oriented for basal slip in these regions of material.

Observation of the material around the crack initiation site reveals that the majority of alpha phase material, including lath α and equiaxed α_p grains, is oriented for either basal or prism slip. A typical crack initiation site is shown in Figure 12. It is believed[7] that the texture of these regions promotes plastic deformation in the crack initiating grains. The likelihood of finding a group of α_p grains with similar crystallographic orientations suitable for basal slip is believed to be higher in these textured regions as opposed to a random area with no preferred (i.e., random) crystallographic texture.[7,17] As shown in Figure 12 the textured regions are as large as 300-500 μm in size, which is the approximate dimension of the initial β grain size.

Random areas, far from the crack initiation sites were sectioned to expose the RD-TD plane as described earlier, and they have been examined using OIM to determine if a preferred crystallographic texture also exists in general microstructural areas. Figure 13 illustrates the texture in a randomly selected region of material. In this image, areas with a high degree of preferred texture suitable for basal and prism slip are observed in the nominal microstructure. These regions of preferred texture correspond to the beta grain texture and morphology. The length scale of these textured regions appears to be 300-500 μm in size, and this is approximately the size of the beta grains, which indicates that these textured regions formed in the initial β processing steps.

Thus, it appears that the presence of a preferred texture suitable for basal and prism slip is a necessary, but not sufficient condition for crack initiation. In these regions of preferred texture, it is clear that the majority of the α phase material shares the same crystallographic orientation. However, the strength of the preferred texture will dramatically affect the resistance to fatigue crack initiation. In other words, a weakly textured region of material will not promote crack initiation and propagation as successfully as a suitably oriented strongly textured region might. It has been established that regions of material with preferred texture for basal and prism slip are found at the crack initiation site. However, quantification of these variations in texture intensity has not been completed and this will be examined in future work.

Thus far, the texture of the α phase, that is the lath α and the α_p grains, has been considered as one. However, the texture of the lath α and equiaxed α_p phases should be considered separately since the correlation in the textures of these phases will affect the ease of slip transmission between grains. The lath α maintain a Burgers orientation relationship with the β phase, whereby the basal (0001) plane of the α phase is parallel to the (110) plane of the β phase.[37] Due to the spherodization process which forms the α_p grains, it is generally assumed that equiaxed α_p are not crystallographically related to the prior β grain orientation.[38] However, Woodfield et. al.[12] note that strains on the order of $\varepsilon = 1$ are required to spheroidize the α laths to form α_p grains, but this strain still may not be high enough to cause recrystallization of the α lath material as they spherodize. Therefore, the α_p grains may in fact share a crystallographic orientation relationship with the prior β and hence the lath α, and slip transmission across phases may not be hindered by the grain boundaries. Quantification of these individual texture components remains as future work.

Figure 14 is a schematic that depicts the proposed mechanism of subsurface fatigue crack initiation that is consistent with the observations in this study. The α_p grains are shown in the schematic, while the lath α is not drawn, but assumed to have the same crystallographic orientation as the α_p grains. The larger grayscale regions are drawn to illustrate the beta grains. Each of the images depict the stages of slip accumulation in α_p grains, which ultimately leads to fatigue crack initiation. Figure 14 (a) illustrates the general microstructure, which is free of deformation and slip accumulation, while (b) depicts the accumulation of slip in a few α_p grains. Figure 14 (c) shows the intensification of slip in those initial grains and the initiation of slip deformation in a few adjacent α_p grains. The last stage, as shown in Figure 14 (d) indicates that a crack has initiated from the linkup of these related slip events. This proposed mechanism is based on the fractographic evidence that crack initiation takes place across a number of α_p grains, typically over a region of 40-70 μm in diameter. The facets that form on the fracture surface result from slip deformation on and eventual separation of the basal plane in α_p grains. Additionally, as shown in Figure 12, it appears that these α_p grains are contained within one large beta grain and that many of them have similar crystallographic orientations. Since the α_p grains share an orientation with each other, it is presumed that if slip can accumulate in one of these grains, it will likely be able to accumulate in a number of α_p grains within the beta grain. Likewise, the lath α are known to be oriented for slip deformation in these regions and are presumed to accumulate slip and contribute to the overall fatigue damage accumulation in these microstructural regions. This mechanism of crack initiation is applicable to all types of initiation sites that were observed. For the macroscopically planar fracture surfaces, the α_p grains and lath α are presumed to be aligned such that the activation of slip in all of the grains occurs across the same macroscopic plane. In the case of isolated facets, the activated slip planes within grains at the crack initiation sites are slightly misaligned with each other and as a result individual facets are observed.

A similar explanation for crack initiation has been postulated in the work of LeBiavant et al.[7] on the microstructural influences of bending fatigue in Ti-6Al-4V. They observed that cracks initiate in macrozones, which are defined as regions of material in which the majority of α_p grains have a similar orientation. In the macrozone that initiated the dominant fatigue crack, multiple microcracks were observed. They postulated that the dominant fatigue crack grew out of these macrozones due to microcrack coalescence. In the current work, there is no evidence of slip offsets or microcracks in α_p grains aside from those on the fracture surface. Fatigue damage is believed to accumulate throughout these similarly oriented regions of material and slip activity in neighboring grains may facilitate crack initiation and growth. However, no evidence of other cracks is observed and thus crack coalescence is not believed to significantly affect crack growth rates. This difference may be due to the fact that LeBiavant et. al.[7] performed their tests at 800 MPa in a material with a yield strength of 850 MPa, while the current investigation focused on the fatigue behavior at much lower stresses in the range of 0.4-0.6 of σ_{YS}. Thus, in this study it is unlikely that slip activity would intensify to such an extent that fatigue cracks would initiate in other α_p grains.

The proposed mechanism can be generalized to explain the process of fatigue crack initiation for the three types of crack initiation sites that were observed. In the case of surface crack initiation, faceted fracture of α_p grains is still observed, and the mechanism

is essentially the same. However, the size of the faceted region is smaller for surface failures than it is for subsurface crack initiation sites. Therefore, the same mechanism is believed to be applicable, but fewer α_p grains are required to accumulate slip, since surface connected cracks can be smaller than subsurface cracks and still propagate at the same rate due to differences in stress intensity and environmental contributions at these sites. In subsurface macroscopically planar failures, the whole faceted region has the same spatial orientation with respect to the loading axis. This indicates that the crack initiation region all has a similar crystallographic orientation. The noticeable feature of these initiation sites is that they appear to form from the faceted fracture of transformed beta regions of material. There are clearly α_p grains in that area, however, the slip planes of α_p grains and transformed beta regions of material must be aligned such that the grain boundaries between these phases are not distinguishable on the fracture surface. For these types of failures, it is still thought that slip must accumulate in a number of α_p grains or transformed beta regions in order to initiate a fatigue crack.

IV. CONCLUSIONS

Ultrasonic fatigue at a load ratio of 0.05 and stresses (σ_{max}) in the range of 500-700 MPa has been shown to produce failures that display similar trends in lifetime and fractographic appearance with respect to conventional frequency fatigue. Cracks initiate in larger than average sized α_p grains through a slip process. The initiation process leads to failure of the α_p grains along the basal plane. Pseudo-cleavage is not operative, since facets are oriented for slip on rational crystallographic planes. Cracks typically form in α_p grains with similar orientations that favor slip on basal planes in which the basal planes are only slightly misaligned in neighboring grains. These microstructural configurations appear to be found more often in textured regions. It is believed that this allows for relatively easy slip transmission between neighboring α_p grains. However, spatial clustering of α_p grains has been proven not to be the distinguishing microstructural feature at crack initiation sites. Crack initiation sites have a preferred texture, and it is observed that a majority of the grains near the site are oriented for easy basal or prism <a> type slip. Analysis of the fatigue lifetime data using probabilistic models of fatigue crack initiation will be presented in a forthcoming paper.

V. ACKNOWLEDGEMENTS

Financial support from AFOSR Metallic Materials Program (Project # F49620-03-1 - 0069) is gratefully acknowledged. One of the authors (CJS) would like to acknowledge funding from the STEP program at the AFRL Materials and Manufacturing Directorate.

Technical assistance from C. Torbet of the University of Michigan is appreciated.

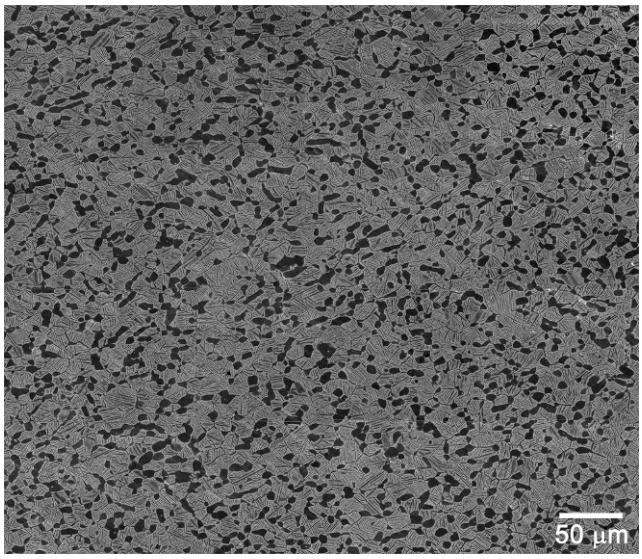

Figure 1. Secondary electron micrograph of a nominal microstructural area that displays the equiaxed α_p grains in a transformed β matrix.

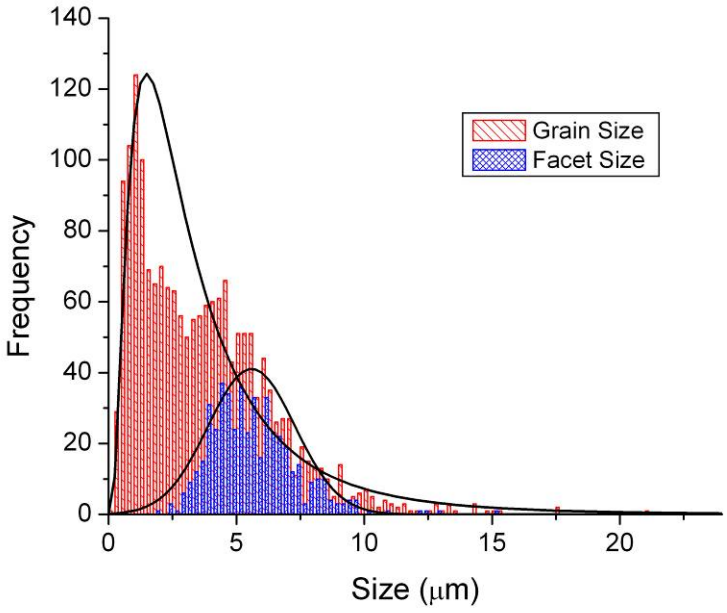

Figure 2. The histogram of α_p grain size and α_p facet size depicts the distribution of feature sizes measured in this investigation.

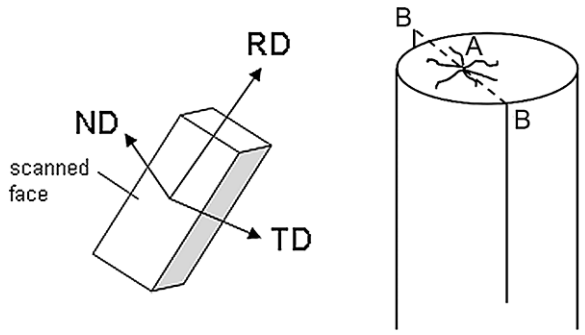

Figure 3. Schematic of sectioning plane for orientation relative to loading axis at crack initiation site. RD corresponds to the loading axis, while plane B-B corresponds to the RD-TD plane.

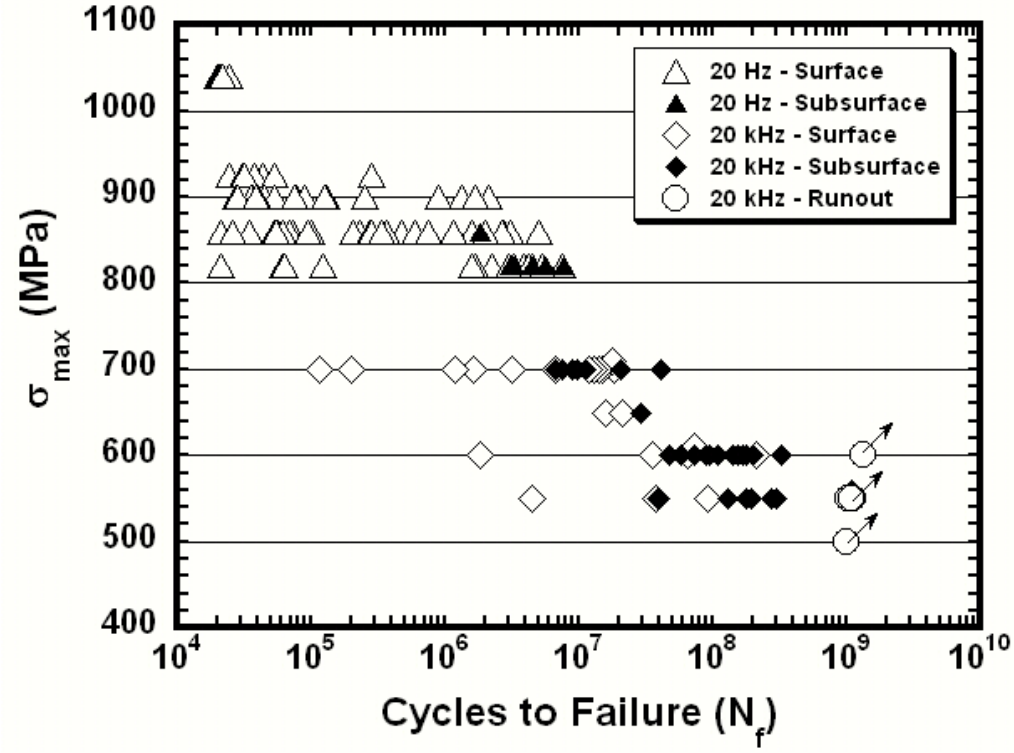

Figure 4. SN curve displaying the fatigue lifetimes of specimens tested at ultrasonic frequencies and conventional frequencies.[23]

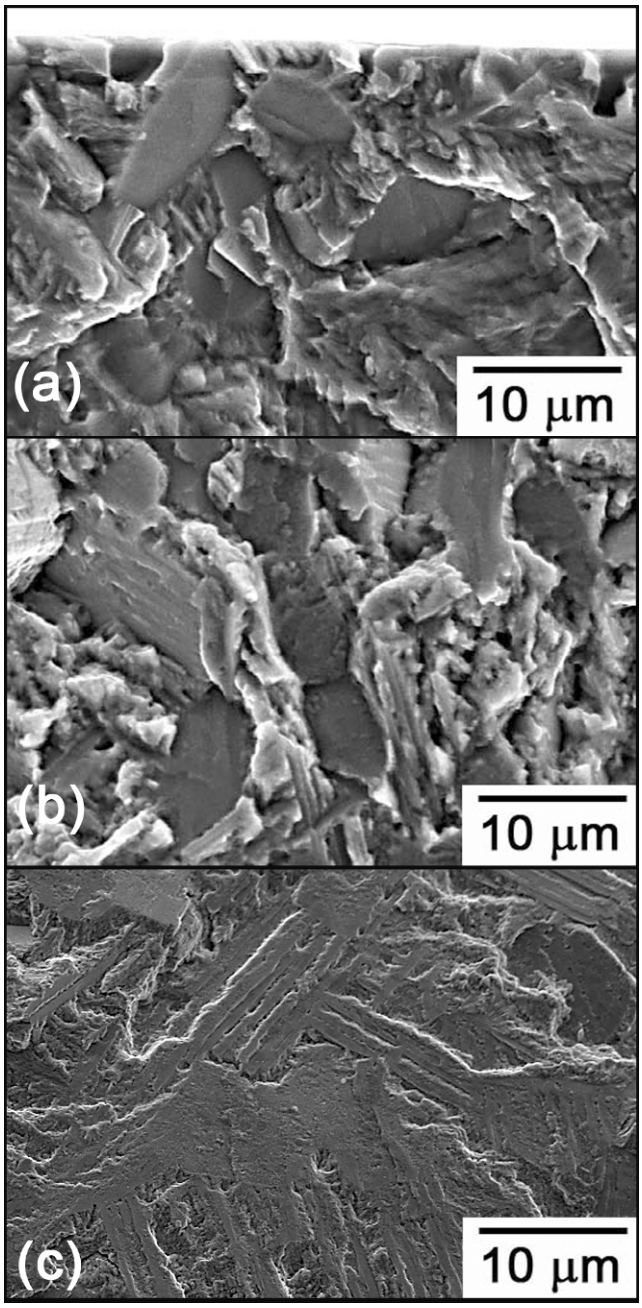

Figure 5. Fractographs displaying examples of the three types of fracture surfaces: (a) surface, (b) isolated subsurface faceting, and (c) macroscopically planar subsurface crack initiation sites.

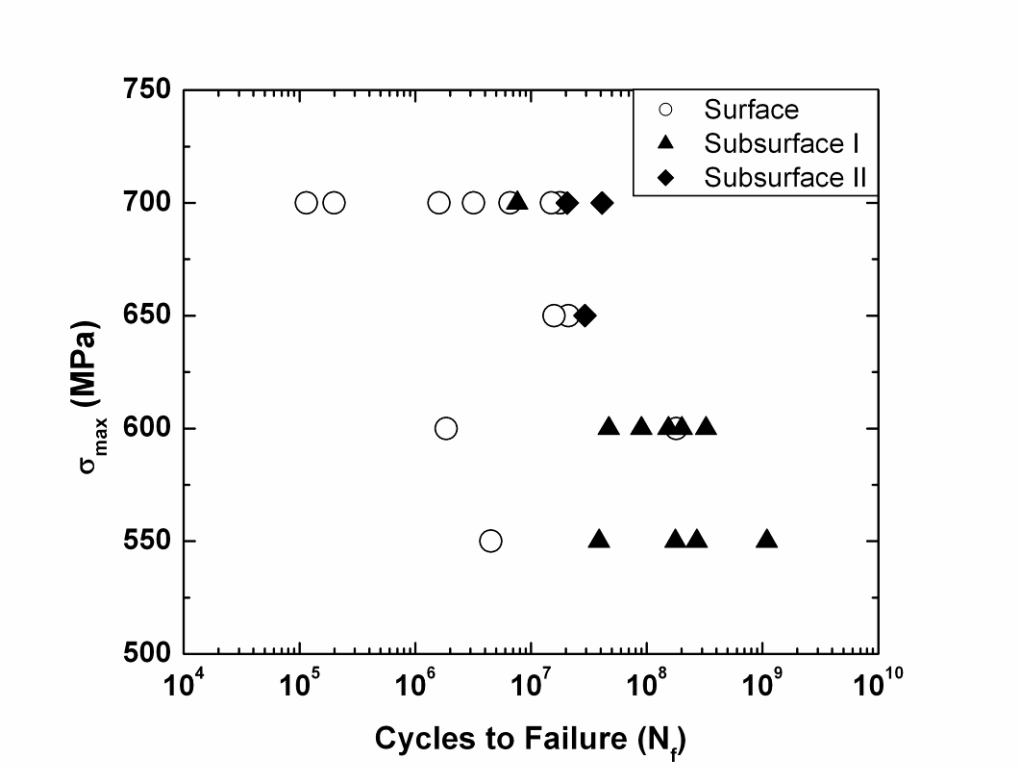

Figure 6. SN curve displaying only ultrasonic frequency (20 kHz) data with initiation types distinguished.

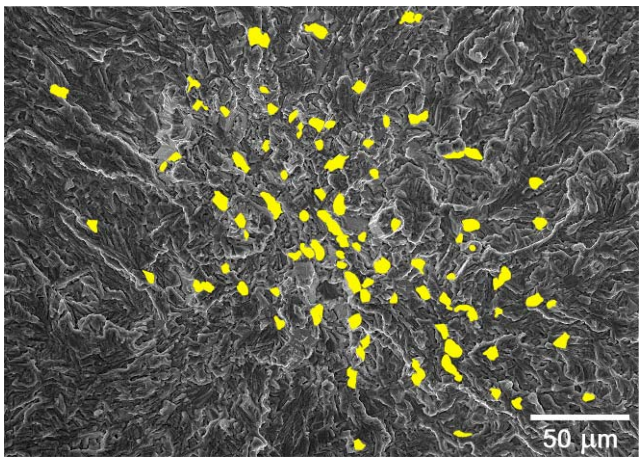

Figure 7. A typical fractograph displaying isolated subsurface faceting where the facets have been highlighted.

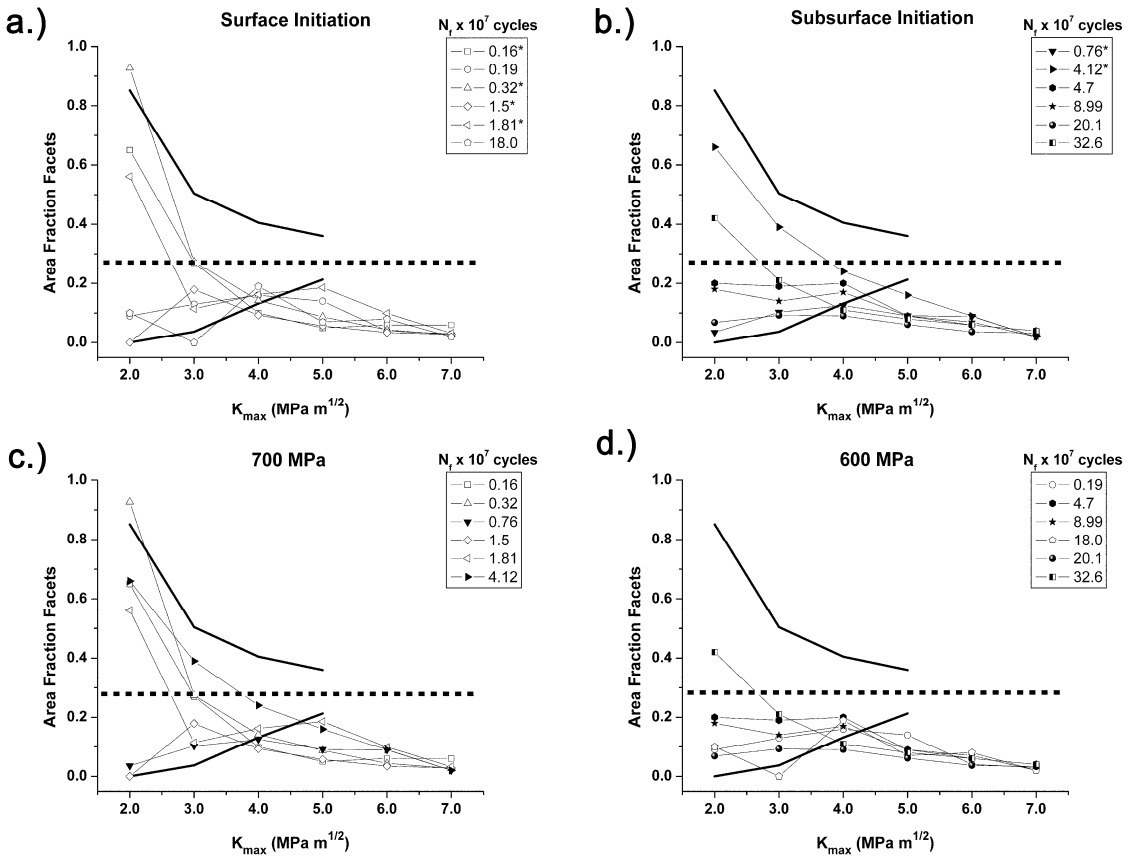

Figure 8. Area fraction clustering plots for (a) surface crack initiation, (b) isolated subsurface faceting, (c) failures from testing at (σ_{max}) 700 MPa, and (d) 600 MPa. The dark bounding lines depict the extremes of spatial orientations of α_p grains within the nominal microstructure.

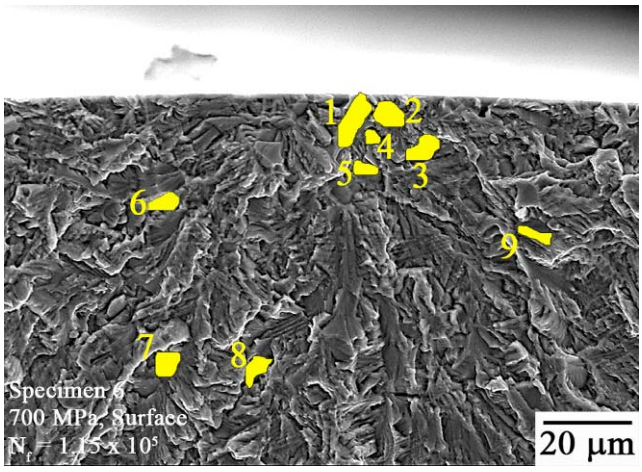

Figure 9. A fractograph indicating the facets that have been measured with MeX.

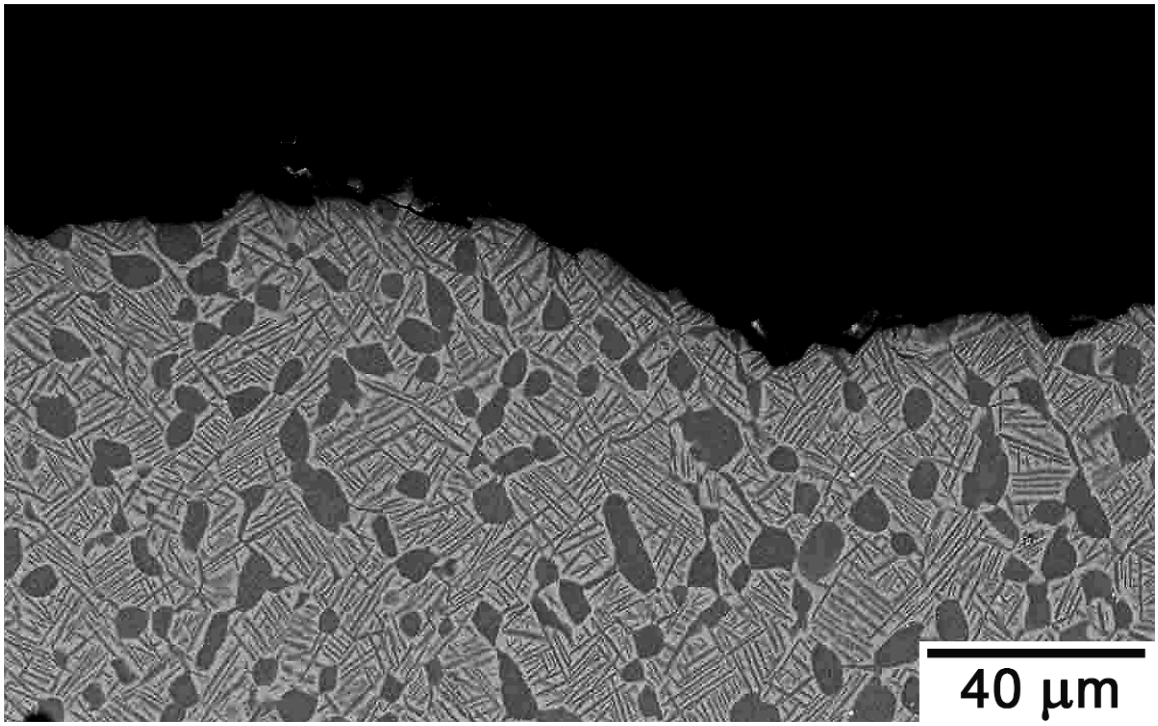

Figure 10. Subsurface crack initiation site after sectioning to expose a plane just below the crack initiation site.

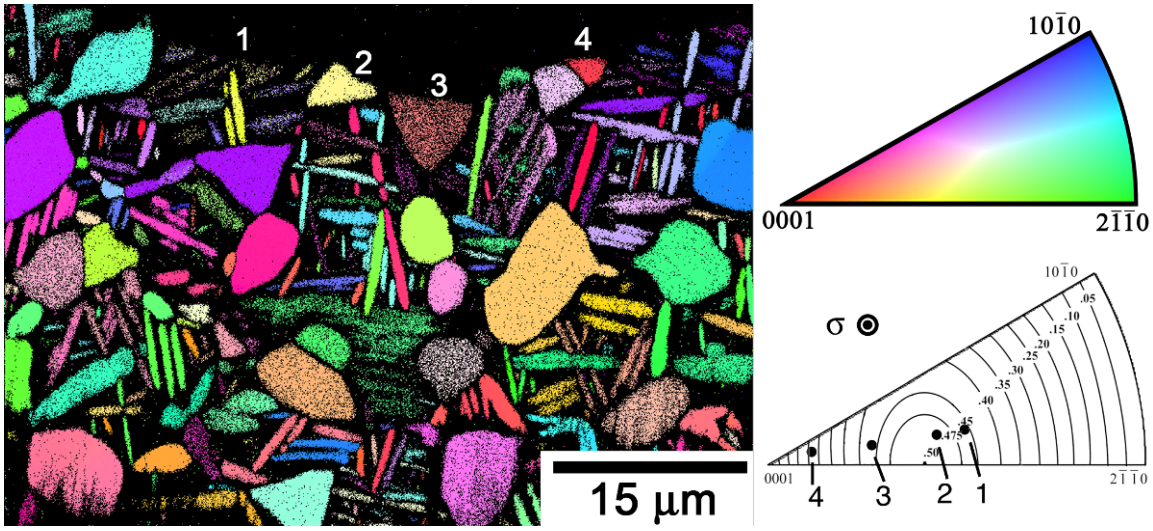

Figure 11. This figure illustrates the crystallographic orientation of α_p grains what have failed by faceted fracture. The spatial orientation of the facet poles have been plotted in the inverse pole figure which also shows the contour lines of the Schmid factor for basal slip.

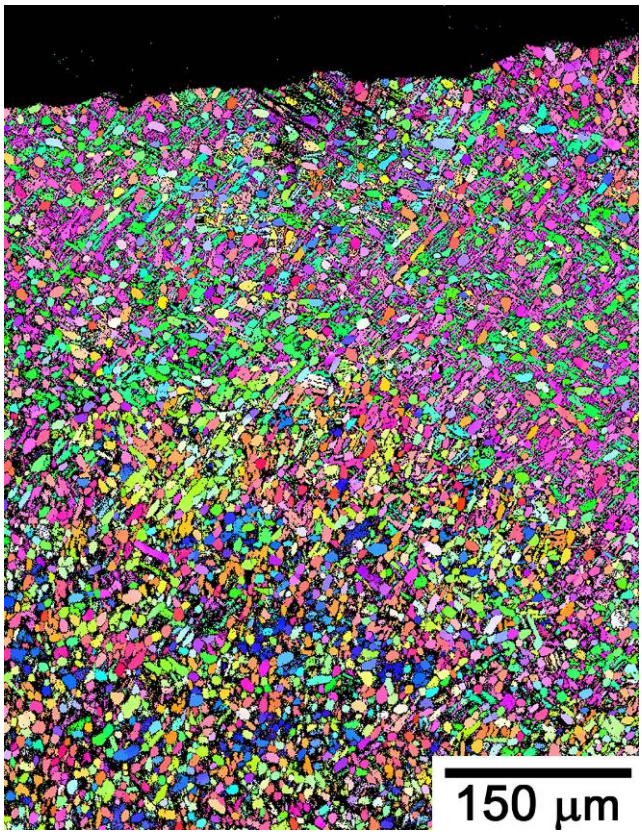

Figure 12. Example inverse pole figure (IPF) map from an OIM scan displaying the texture of the α phase near the crack initiation site.

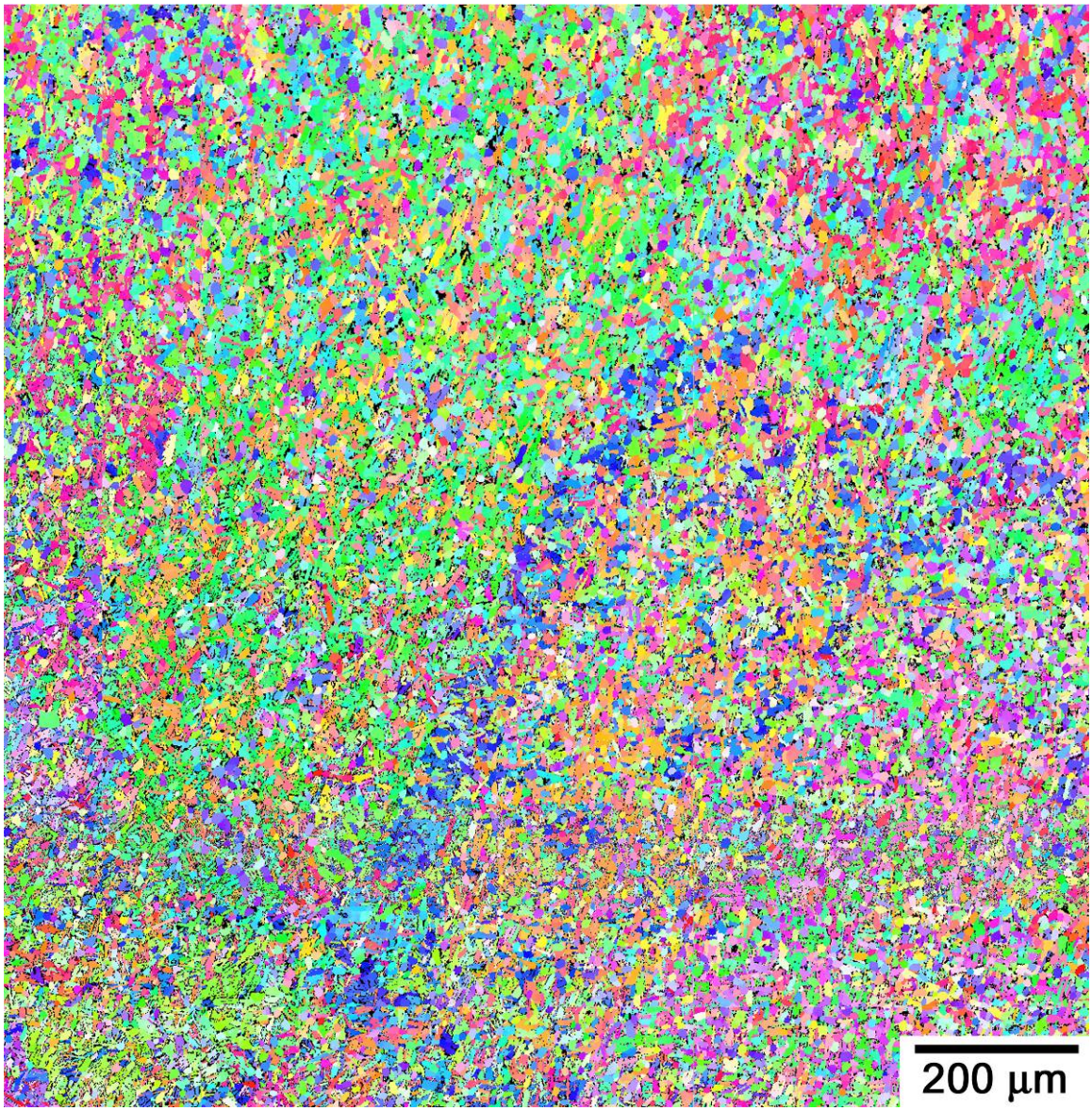

Figure 13. A typical IPF map from an OIM scan that illustrates large regions of similarly oriented material are commonly found in the general microstructure.

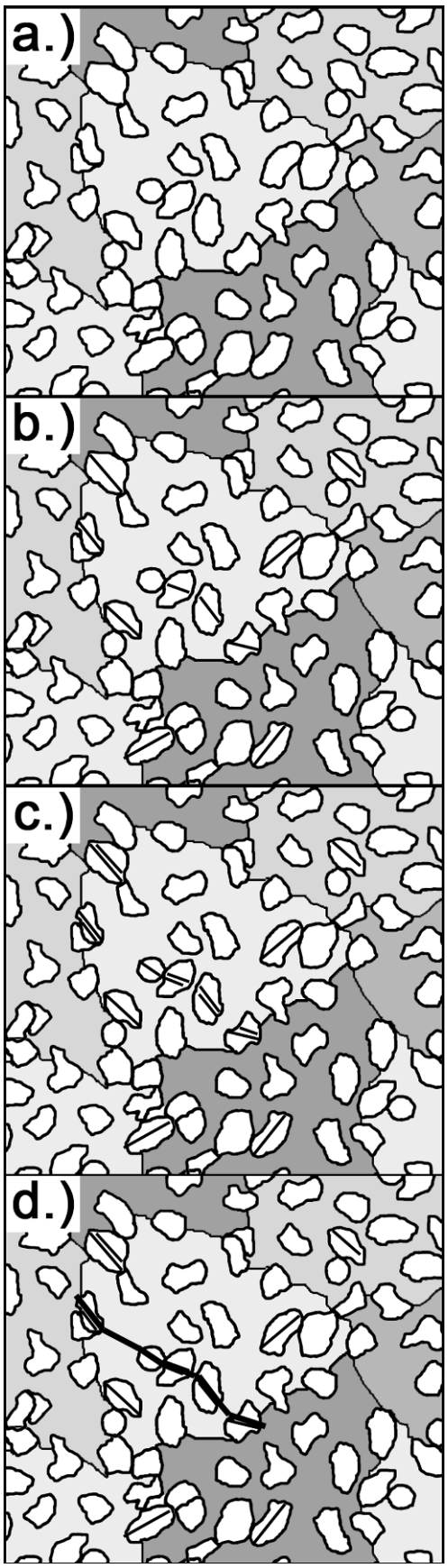
a.)
b.)
c.)
d.)

Figure 14. A schematic depiction of the crack initiation process. a.) illustrates the microstructure before any fatigue cycles have been applied. b.) depicts slip accumulation in a few favorably oriented α_p grains. c.) demonstrates the intensification of slip within ceratin α_p grains and slip accumulation within neighboring grains as well. d.) illustrates the formation of a crack within the microstructure.

Table I. Spatial orientation of facets with respect to fracture surface (in degrees).

Facet #	**1**	**2**	**3**	**4**	**5a**	**5b**	**6**	**7**	**8**	**9**
Angle	**46**	**45**	**39**	**19**	**26**	**35**	**33**	**31**	**32**	**21**

Table II. Orientation of facets (in degrees).

Facet #	**1***	**2**	**3**	**4**
Spatial Orientation (w.r.t.) Tensile Axis)	**44**	**42**	**25**	**15**
Crystallographic Orientation (w.r.t. [0001])	**55**	**48**	**30**	**13**

[1] C. Engler-Pinto, Jr., R. Frisch, Sr., J. Lasecki, H. Mayer, J. Allison: In VHCF4; Eds. J. Allison, J.W.Jones, J. Larsen, R. Ritchie, 2007 TMS, Warrendale, PA, pp. 421-427.

[2] C. Bathias: Fatigue Fract. Eng. Mat. Struct., 1999, **22**, pp. 559-565.

[3] S. Nishijima, K. Kanazawa: Fatigue Fract. Eng. Mat. Struct., 1999, **22**, pp. 601–607.

[4] H. Mughrabi: Fatigue Fract. Eng. Mat. Struct., 1999, **22**, pp. 633-641.

[5] P. Lukáš, L. Kunz: Fatigue Fract. Eng. Mat. Struct., 1999, **22**, pp. 747-753.

[6] Y. Murakami, T. Nomoto, T. Ueda: Fatigue Fract. Eng. Mat. Struct., 1999, **22**, pp. 581-590.

[7] K LeBiavant, S Pommier, C Prioul: Fatigue Fract. Eng. Mat. Struct., 2002, **25**, pp. 527-545.

[8] J.A. Hall: Int. J. Fatigue, 1997, **31** Suppl. 1, S23.

[9] Y. Mahajan, H. Margolin: Metall. Trans. A, 1982, **13A**, pp. 257-268.

[10] K.S. Ravi Chandran, S.K. Jha: Acta Mat., 2005, **53**, pp. 1867-1881.

[11] D. L. Davidson, R.G. Tryon, M. Oja, R. Matthews, K.S. Ravi Chandran: Metall. Trans. A, 2007, **38A**, pp. 2214-2225.

[12] A. P. Woodfield, M.D. Gorman, R.R. Corderman, J.A. Sutliff, B.Yamrom: In Titanium ’95 Eds. P.A. Blenkinsop, W.J. Evans, H.M. Flower, IOM, 1996, pp.1116-1123.

[13] T.R. Bieler, S.L. Semiatin: Int. J. Plasticity, 2002, **18**, pp. 1165-1189.

[14] G. Lütjering: Mat. Sci. Eng., 1998, **A243**, pp. 32-45.

[15] A.W. Bowen: Acta Metall., 1975, **23**, pp. 1401-1409.

[16] I. Bantounas, T. Lindley, D. Rugg, D. Dye: Acta Mat., 2007, **55**, pp. 5655-5665.

[17] V. Sinha, J.E. Spowart, M.J. Mills, J.C. Williams: Metall. Mat. Trans. A, May 2006, **37A**, pp.1507-1518.

[18] G. Lutjering and J.C. Williams: Titanium, Springer-Verlag, Berlin, Heidelberg, 2003, pp.182-185.

[19] J.M. Larsen, J.R. Jira, K.S. Ravi Chandran: In Small Crack Test Methods, ASTM STP 1149, JM Larsen and JE Allison, Eds., ASTM, Philadelphia, PA, 1992, pp.57-80.

[20] A. Shyam, C.J. Torbet, S.K. Jha, J.M. Larsen, M.J. Caton, C.J. Szczepanski, T.M. Pollock, J.W. Jones: In Superalloys 2004, Eds. K.A. Green, T.M. Pollock, H. Harada, T.E. Howson, R.C. Reed, J.J. Schirra, S. Walston; TMS, 2004, pp. 259-268.

[21] C. J. Szczepanski; A. Shyam; S. K. Jha; J. M. Larsen; C. J. Torbet; S. J. Johnson; J. W. Jones: In Materials Damage Prognosis, Eds. J.M. Larsen, L. Christodoulou, J.R. Calcaterra, M.L. Dent, M.M. Deriso, W.J. Hardman, J.W. Jones and S.M. Russ. TMS 2005, pp. 315-320.

[22] J.Z. Yi, C.J. Torbet, Q. Feng, T.M. Pollock, J.W. Jones: Mat. Sci. Eng., 2007, **A443**, pp. 142-149.

[23] S.K. Jha, J.M. Larsen, A.H. Rosenberger, G.A. Hartman: Scripta Mat., 2003, **48**, pp. 1637-1642.

[24] C.J. Szczepanski, S.K. Jha, J.M. Larsen, J.W. Jones: In VHCF4; Eds. J. Allison, J.W.Jones, J. Larsen, R. Ritchie, 2007 TMS, Warrendale, PA, pp.37-44.

[25] M. Papakyriacou, H. Mayer, C. Pypen, H. Plenk, Jr., S. Stanzl-Tschegg: Mat. Sci. Eng., 2001, **A308**, pp. 143-152.

[26] J. Mendez, S. Mailly, P. Villechaise: In Temperature-Fatigue Interactions, Eds. L. Remy, J. Petit. ESIS TTP 29. Elsevier, Amsterdam, 2002, pp. 95-102.

[27] H. Mughrabi: Fatigue Fract. Eng. Mat. Struct., 2002, **25**, pp.755-764.

[28] S.K. Jha and J.M. Larsen: In VHCF4; Eds. J. Allison, J.W.Jones, J. Larsen, R. Ritchie, 2007 TMS, Warrendale, PA, pp.385-396.

[29] J.L. Gilbert, H.R. Piehler: Metall. Trans. A, March 1993, **24A**, pp. 669-680.

[30] J.C. Newman, Jr., I.S. Raju: Eng. Fract. Mech., 1981, **15**, pp. 185-192.

[31] Y. Murakami: "Stress intensity factors handbook," Oxford; New York: Pergamon, 1987, p.668.

[32] D.L. Davidson, D. Eylon: Metall. Mat. Trans. A, May 1980, **11A**, pp. 837-843.

[33] J.A. Ruppen, D. Eylon, A.J. McEvily: Metall. Mat. Trans. A, June 1980, **11A**, pp. 1072-1075.

[34] R.K. Nalla, B.L. Boyce, J.P. Campbell, J.O. Peters, R.O. Ritchie: Metall. Mat. Trans. A, March 2002, **33A**, pp. 899-918.

[35] D.F. Neal, P.A. Blenkinsop: Acta Metall., 1976, **24**, pp. 59-63.

[36] W.J. Evans, M.R. Bache: Int. J. Fat., 1994, **16,** pp. 443-452.

[37] W.G. Burgers, Physica, 1934, **1**, pp. 561-586.

[38] H. Margolin, J.C. Williams, J.C. Chesnutt, G. Lutjering: In Titanium '80 Proc. Fourth Int. Conf. on Titanium, Eds. H. Kimura, O. Izumi, Met. Soc. AIME, 1980, pp. 169-216.